

Size Dependence of Blackbody Radiation Induced Hydrogen Formation in $\text{Al}^+(\text{H}_2\text{O})_n$ Hydrated Aluminum Cations and Their Reactivity with Hydrogen Chloride

Martin Beyer, Uwe Achatz, Christian Berg,[†] Stefan Joos, Gereon Niedner-Schatteburg, and Vladimir E. Bondybey*

Institut für Physikalische und Theoretische Chemie, Technische Universität München, Lichtenbergstraße 4, 85747 Garching, Germany

Received: September 14, 1998; In Final Form: November 30, 1998

Trapped hydrated aluminum cluster ions are studied by FT-ICR mass spectrometry on a time scale of several seconds. Blackbody radiation, besides causing the fragmentation of the cluster by stepwise loss of individual water molecules, induces in hydrated aluminum clusters $\text{Al}^+(\text{H}_2\text{O})_n$ an intracuster reaction yielding hydrated hydroxide and releasing molecular hydrogen. Local deviations of the individual rate constants for the water loss process from a linear size dependence are due to increased rigidity of certain sizes due to the formation of stabilizing hydrogen-bonded bridges. In comparison with previously studied hydrated ions, surface versus internal solvation is discussed. The preferential occurrence of the intracuster reaction in the size region of $n = 11\text{--}24$ is attributed to a concerted proton-transfer mechanism, in which a chain of at least two water molecules is needed to transfer a proton between two first solvation shell water molecules, leading to formation of an $\text{Al}(\text{OH})_2^+(\text{H}_2\text{O})_n$ hydrated aluminum dihydroxide cation and molecular hydrogen. The $\text{Al}^+(\text{H}_2\text{O})_n$ species with $n \geq 13$ and all investigated $\text{Al}(\text{OH})_2^+(\text{H}_2\text{O})_m$ species are able to react with and “dissolve” HCl. The maximum number of HCl molecules in the cluster strongly depends on the number of water molecules available for solvation. The presence of HCl in the cluster removes the upper limit for the intracuster reaction, which leads to the formation of molecular hydrogen, driven by blackbody radiation. This is taken as further evidence for the validity of the proton-transfer mechanism.

Introduction

Solvated metal cations are ideal model systems for understanding solution chemistry, and their solvation^{1–5} and hydration^{6–13} were therefore extensively studied in the past decade. High-pressure mass spectrometry and collision-induced dissociation studies can yield information about the thermochemistry of solvated ions,^{6,7,12} while insight into the structure and stepwise formation of the hydration shells can be obtained from spectroscopic¹⁴ and computational^{11,12} studies. Only much more recently it was realized that ionized water clusters and hydrated ions can serve as “microsolutions” for direct studies of condensed-phase reactions. Thus, hydrated H^+ or OH^- ions can, similar to protons or hydroxide anions in solutions, promote acid- or base-catalyzed chemical reactions¹⁵ and can be used as a medium for studies of various solution reactions^{16,17} or even as model systems for polar stratospheric clouds.¹⁸ Investigations of the reactions of solvated metal ions bring gas-phase work closer to the conditions of catalysis in the bulk.¹⁹ Special emphasis is laid on the investigation of intracuster reactions,^{20–25} in which the presence of the ion causes a chemical reaction between the solvent molecules.

Very thoroughly investigated were hydrated magnesium ions and the formation of atomic hydrogen in $\text{Mg}^+(\text{H}_2\text{O})_n$. Fuke and co-workers^{20a,b} noted in their molecular beam experiment that

while for smaller clusters hydrated hydroxide, $\text{MgOH}^+(\text{H}_2\text{O})_m$, clusters were formed, above $n \approx 17$ the composition changes to $\text{Mg}^+(\text{H}_2\text{O})_n$. A more complete picture can be gained from an FT-ICR experiment, and we were able to demonstrate that under the influence of room-temperature blackbody radiation^{26–30} the larger $\text{Mg}^+(\text{H}_2\text{O})_n$ clusters fragment and, in the size region $n \approx 16\text{--}21$, interconvert to the $\text{MgOH}^+(\text{H}_2\text{O})_m$ hydroxide species by the loss of atomic hydrogen.²¹ To elucidate the mechanism for these reactions, it was proposed that the $\text{Mg}^+(\text{H}_2\text{O})_n$ species actually exist as an Mg^{2+}/e^- hydrated ion pair.^{20,21} As the larger clusters shrink due to blackbody radiation induced fragmentation, the number of water molecules available is insufficient to stabilize the ion pair, and it may recombine forming the much more reactive, open-shell Mg^+ species, which then reacts with a water ligand forming hydroxide and freeing a hydrogen atom. When HCl is introduced into the cluster, a similar process occurs.²¹ The HCl molecule is presumably dissolved into H^+ and Cl^- , with the proton recombining with the hydrated electron. The energy liberated in the process leads to loss of the hydrogen atom along with one or two water ligands.

An enhanced understanding of the interaction of water with metals is highly desirable for many reasons. The formation of nascent hydrogen in solution is of considerable interest since hydrogen is expected to play a key role in the world's energy supply of the future. Interaction of water with a metal surface is usually the first step in corrosion processes. Specifically, for aluminum, some 50 tons of the metal and its oxides and hydroxides is dispersed in the atmosphere with each launch of

* Corresponding author. Fax: ++49-89-289-13416. E-mail: bondybey@ch.tum.de.

[†] Current address: Bruker Analytical Systems, Inc., 15 Fortune Drive, Billerica, MA 01821.

the space shuttle,³¹ and its fate is certainly of some concern. Aluminium–water clusters and their ions have been studied by photoionization and photodissociation.³² To learn more about the chemistry of hydrated aluminum species, we have investigated the blackbody radiation induced fragmentation of $\text{Al}^+(\text{H}_2\text{O})_n$ hydrated aluminum cations, with special emphasis on the effect of the change in electronic configuration of the metal ion on the intracuster reactions, as compared to magnesium. In our previous report,²² we have observed the formation of hydrated aluminum–dihydroxide species $\text{Al}(\text{OH})_2^+(\text{H}_2\text{O})_m$ and evaporation of molecular hydrogen in a size regime of $n \approx 12$ –24 water molecules. Two mechanisms were proposed, an insertion of the aluminum into an O–H bond and a concerted proton-transfer mechanism. To gain more information in favor or against these or other more speculative mechanisms, like the clathrate and double hydrated electron hypothesis,^{21a} we undertook additional experiments that will be reported in this publication. The size dependence of the hydrogen formation reaction was examined by determining the rate constants of the blackbody radiation induced dissociation of size-selected $\text{Al}^+(\text{H}_2\text{O})_n$ clusters. Reactions of $\text{Al}^+(\text{H}_2\text{O})_n$ with HCl will yield additional insight into the behavior of $\text{Al}^+(\text{H}_2\text{O})_n$ hydrated aluminum ions.

Experimental Section

The experiments are performed on a modified FT-ICR Spectrospin CMS47X, equipped with a 4.7 T magnet and an additional source chamber with a laser vaporization source, described in detail elsewhere.³³ Briefly, hydrated metal ions are produced by laser vaporization³⁴ of a solid disk of aluminum (Chempur, 99.999%+) and expansion of the plasma into a high vacuum by a 50 μs pulse of helium (Messer Griesheim 4.6), which was seeded with water vapor at a partial pressure of 25 mbar. The ions were accelerated, transferred through four differential pumping stages by electrostatic lenses, decelerated, and stored in the ICR cell at a pressure of $\sim 4 \times 10^{-10}$ mbar. To measure rate constants of size-selected ions, unwanted peaks were ejected by single frequency pulses in a mass range of 90 mass units to lower and 72 mass units to higher masses around the peak of interest. Mass spectra were taken at typically 12 different reaction delays, and the relative intensities of reactant and product ions fit to first-order reaction kinetics. Reactant gas HCl (Aldrich 99%) was introduced through leak valves at a calibrated pressure of 1.2×10^{-7} mbar.

Results and Discussion

Blackbody Radiation Induced Fragmentation of Size-Selected $\text{Al}^+(\text{H}_2\text{O})_n$. Similar to other solvated ions, the hydrated aluminum clusters gradually fragment due to absorption of infrared blackbody radiation. We have examined reactions of size-selected clusters in the size range of $n = 3$ –45 as a function of reaction time to extract the first-order rate constants. Typical data for $n = 21$ is shown in Figure 1, showing the $\text{Al}^+(\text{H}_2\text{O})_{21}$ cluster peak immediately after selection and after reaction delays of 0.15 and 0.3 s. Unlike for larger clusters, for $n = 21$ a simple loss of a single water molecule is observed only to a small extent, with the loss of an H_2 molecule and formation of an $\text{Al}(\text{OH})_2^+(\text{H}_2\text{O})_{16,17}$ hydrated aluminum dihydroxide cation being the major process. In this reaction, aluminum formally changes its oxidation state from +1 to +3, retaining a closed-shell electron configuration. The formation of the aluminum dihydroxide ion and molecular hydrogen is exothermic enough to cause the evaporation of two or three water molecules, which places its enthalpy in the range of $\Delta H = -150$ to -50 kJ/mol.

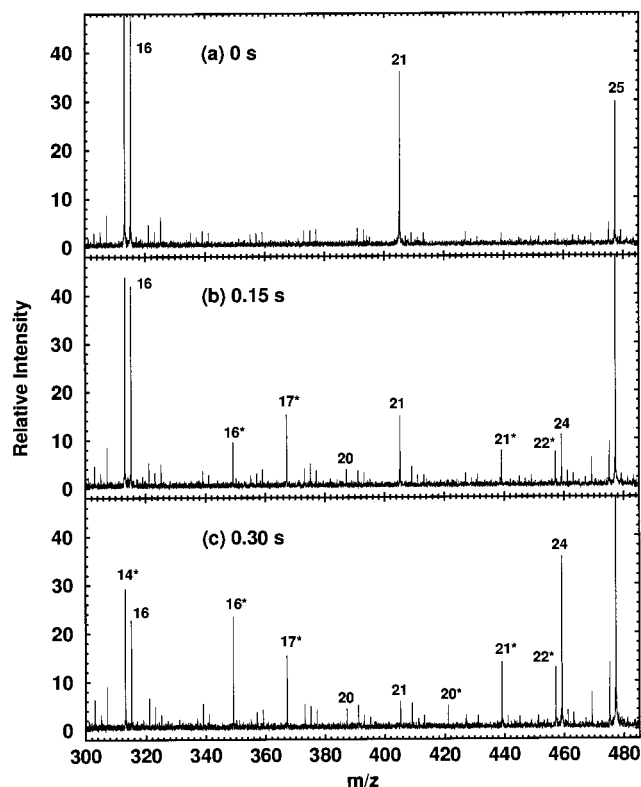


Figure 1. Mass spectra of the blackbody radiation induced unimolecular reactions of size-selected $\text{Al}^+(\text{H}_2\text{O})_{21}$ with a delay of (a) 0 s, (b) 0.15 s, and (c) 0.3 s after trapping. A rather small fraction of the clusters fragment to $\text{Al}^+(\text{H}_2\text{O})_{20}$; the major part undergoes an intracuster reaction to form $\text{Al}(\text{OH})_2^+(\text{H}_2\text{O})_{16,17}$ with a concomitant loss of two or three water molecules, respectively. The numbers denote $\text{Al}^+(\text{H}_2\text{O})_n$ hydrated aluminum species, numbers with a star indicate $\text{Al}(\text{OH})_2^+(\text{H}_2\text{O})_m$ hydrated aluminum dihydroxide clusters. The small unlabeled peaks are hydrated $[\text{Al}_2(\text{OH})_m(\text{H}_2\text{O})_n]^+$ species and protonated water clusters, which do not interfere with the experiment.

The first and second H_2O seem to be lost instantaneously on the ICR time scale, i.e., faster than a few milliseconds, since no traces of $\text{Al}(\text{OH})_2^+(\text{H}_2\text{O})_{18,19}$ are observed. The loss of a third water molecule is considerably slower and less efficient, as the $\text{Al}(\text{OH})_2^+(\text{H}_2\text{O})_{17}$ peak is the dominant primary product.

Such size-selected measurements were carried out for all clusters from $n = 3$ –45, and the resulting first-order reaction rates are summarized in Figure 2. The solid black circles show the rate of ligand loss from the $\text{Al}^+(\text{H}_2\text{O})_n$ clusters. The $\text{Al}^+(\text{H}_2\text{O})_3$ cluster fragments only very slowly, resulting in traces of $\text{Al}^+(\text{H}_2\text{O})_2$ after a 20 s reaction delay. One observes the expected overall linear n dependence,^{16,21,26,30} but with a deep minimum between $n \approx 18$ –22. This minimum is due to a competition between loss of water and the efficient intracuster chemical reaction and hydrogen evolution. The rates of this competing reaction are indicated by the hollow squares. The plot shows the total dehydrogenation rate; that is, the rate constants for the two and three water ligand loss were summed up. The dominant feature of this plot is the gradual onset of hydrogen formation at $n = 11$ and its abrupt and complete disappearance at $n = 24$. Also, the details of the size dependence are interesting; the H_2 loss becomes dominant for $n = 13$, but plays only a minor role for $n = 14$ –16, rises then again steeply to a pronounced maximum around $n = 20$ –21, only to disappear again for $n = 24$.

A linear regression of the fragmentation rate constants of those clusters that do not exhibit the intracuster reaction, that

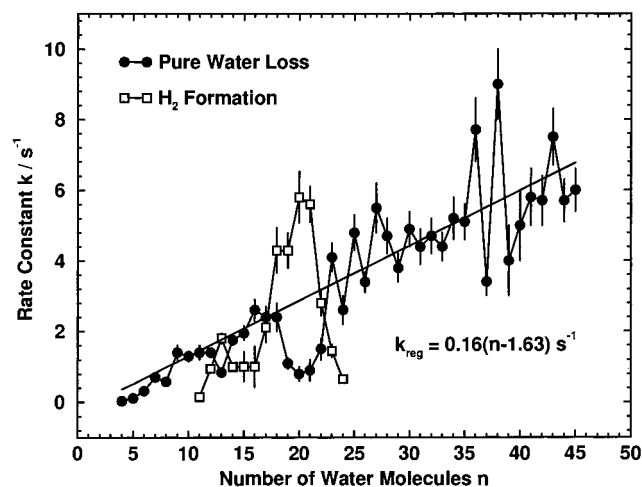


Figure 2. First-order rate constants of the blackbody radiation induced unimolecular reactions of size-selected Al⁺(H₂O)_n. Filled circles denote evaporation of a single water molecule and open squares show the intracuster reaction to form Al(OH)₂⁺(H₂O)_m hydrated aluminum dihydroxide species and H₂ molecular hydrogen with a concomitant loss of two to three water molecules. The intracuster reaction is confined to a size region of 11–24 water molecules, with a pronounced maximum around $n = 20$. For cluster sizes that do not exhibit hydrogen formation, the rate constants of water loss follow an overall linear increase with cluster size with a slope of 0.16 s^{-1} . Where the intracuster reaction reaches its maximum, it is considerably faster than what one would expect for the pure water loss. An interesting “oscillation” fast–slow–fast–slow of the water loss rate constants is observed at $n = 36$ – 39 , which suggests the existence of size regions with rigid, defined structures.

is, for $n = 4$ – 10 and $n = 25$ – 45 , is included in Figure 2 as the solid black line.^{16,21,26,30} It has a slope of 0.16, which agrees reasonably well with the previously obtained value of 0.17 for hydrated magnesium cations,²¹ indicating that the specific nature of the central ion plays only a minor role.

Interestingly, while there are regions where the rate constants follow closely the linear regression, e.g., $n = 4$ – 10 and $n = 29$ – 35 , in others significant deviations can be seen. For instance, between $n = 23$ – 27 and in particular $n = 36$ – 39 they exhibit pronounced oscillations around the linear regression line. A similar observation was made for hydrated magnesium cations,²¹ albeit with slightly shifted values, e.g., with the most pronounced oscillations at $n = 38$ – 41 , while the H⁺(H₂O)_n protonated water clusters²⁶ exhibit oscillations around the “magic” $n = 55$ cluster, $n = 52$ – 56 . This behavior may be rationalized by changes in the internal structure and rigidity of the clusters. If one, in fact, attempts to construct models of the hydrated clusters using ball-and-stick molecular modeling sets, one inevitably ends up with transitions between relatively neat, closed, and rigid geometries to much more floppy, irregular structures. Evaporation of a water molecule from a floppy site of the cluster may proceed as shown schematically in Figure 3a. The H₂O molecule to evaporate leaves a chain of water molecules by a rearrangement of hydrogen bonds, and it evaporates when the remaining hydrogen bond is broken. The energy required for evaporation consists of the energy of the hydrogen bond and the reorganization energy of the cluster, which may be positive or negative. Quite differently may proceed the sequential evaporation of two water molecules from a rigid cluster site depicted in Figure 3b. In this proposed mechanism, the first H₂O leaves a gap in the chain, which cannot be closed because the structure of the cluster does not allow the necessary rearrangement, and two hydrogen bonds have to be broken. Evaporation of the second water molecule requires the breaking of only one hydrogen bond. Two bridges

such as this may cause the oscillating feature at $n = 36$ – 39 in Figure 2. The breaking of two hydrogen bonds would thus correspond to low rate constants; high rate constants would relate to the breaking of one hydrogen bond.

The linear regression line would then be representative of clusters with the distribution of isomers statistical with respect to the mechanism of the evaporation and the number of hydrogen bonds that have to be broken. In the region with the most pronounced deviations, $n = 36$ – 39 , the rate constants oscillate with more than a factor of 2 between the higher and the lower values. Thus, one can envision that, in this size region, the cluster ensembles exhibit relatively defined structures with only a small number of isomers, which require the breaking of either one or two hydrogen bonds for evaporation of a water molecule.

Also, the rate constants of the small clusters may carry some useful information on structural properties of the Al⁺(H₂O)_n species. One may argue that, for example, the relatively stable Al⁺(H₂O)₄ cluster indicates that four water molecules mark the filling of the first solvation shell and that Al⁺ be tetraordinated.^{21a} A subject of a lively ongoing discussion is the hydrated iodide and other anion clusters and the question of “internal” or “surface” solvation.^{16,35,36} While the surface solvation should be less of an issue for the solvation of cations, and one might expect the polar water molecules to readily “wet” the strongly interacting metal cations, recent computational studies by Bauschlicher et al.¹¹ as well as Watanabe et al.¹² came to the conclusion that Al⁺(H₂O)₄ is a case of surface solvation. Their results suggest that there are water molecules present in the second solvation shell before the first is filled so that the cluster can be viewed as the aluminum ion sitting on the “surface” of a water tetramer cluster. Even though this result appears quite surprising in view of the much stronger Al⁺–OH₂ interaction compared with a hydrogen bond in water clusters, it seems to cast some doubt upon special cluster stability being a reliable indicator of shell closure. In any event, metal cations are solvated differently from halides, and the critical size for “internal” solvation, if any, is surely much earlier reached than that for the anions. In fact, the oscillatory behavior of the water loss rate constants is suggestive of internal solvation, with the central ion imposing a rigid structure on the cluster. Unfortunately, the information on the fragmentation behavior in the region of smaller clusters between $n = 11$ and $n = 23$ is obscured by the competitive intracuster chemical reaction.

For clusters below $n = 11$, the only strong deviation from a smooth fragmentation behavior is a sharp rate increase between $n = 8$ and 9. Interestingly, the plots of the rate constants of Al⁺(H₂O)_n and MgOH⁺(H₂O)_{n-1}, which differ, besides the core ion, by only one hydrogen atom, run quite parallel from $n = 6$ to 9, as shown in Figure 4. This points to some common structural features, and this size region seems to be a promising target for spectroscopic, ab initio, or molecular dynamics studies.

The fragmentation process ends when a cluster, which has reached a thermal equilibrium with the blackbody wall radiation, does not have sufficient internal energy to evaporate a water molecule. Dalleska et al.¹³ calculated the internal vibrational energy of an Al⁺(H₂O)₄ cluster with three water molecules directly bound to the metal ion to be $23 \pm 4 \text{ kJ/mol}$ at room temperature. This lies significantly below the measured binding energy of the fourth water molecule to Al⁺ of 60 kJ/mol ,¹³ resulting in a long lifetime of the cluster. On the time scale of the ICR experiment, however, the Boltzmann distribution tail

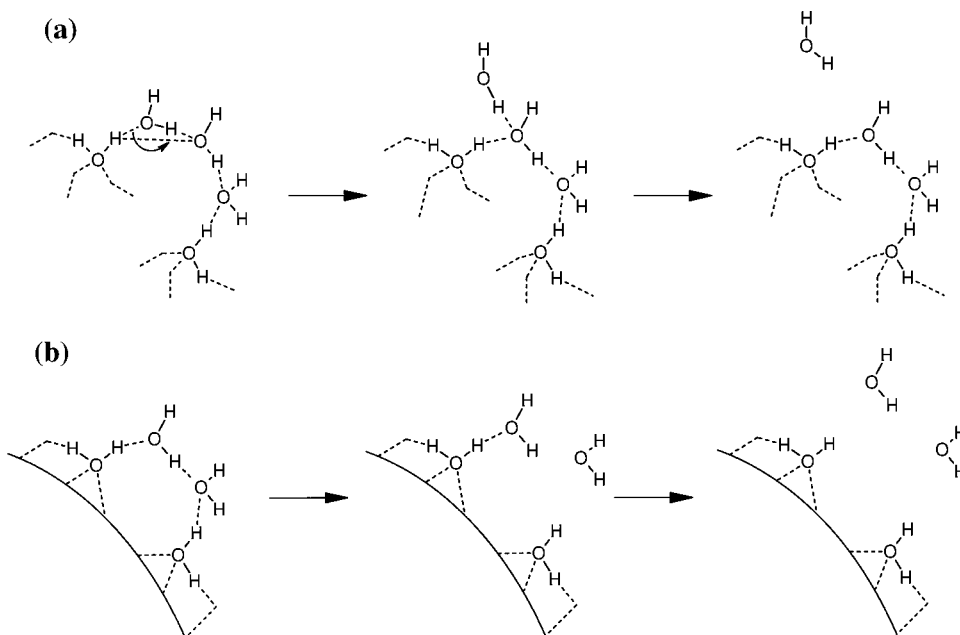


Figure 3. (a) Proposed mechanism for the evaporation of a water molecule from a floppy site of the cluster. H_2O leaves the chain of water molecules by a rearrangement of hydrogen bonds, and it evaporates when the remaining hydrogen bond is broken. (b) Proposed mechanism for the sequential evaporation of two water molecules from a rigid cluster site. The first H_2O leaves a gap in the chain, that cannot be closed because the structure of the cluster does not allow the necessary rearrangement. Two hydrogen bonds have to be broken, resulting in a low rate constant. Evaporation of the second water molecule requires only one hydrogen bond to be broken, leading to a high rate constant. Two bridges such as this may cause the oscillating feature at $n = 36\text{--}39$ in Figure 2.

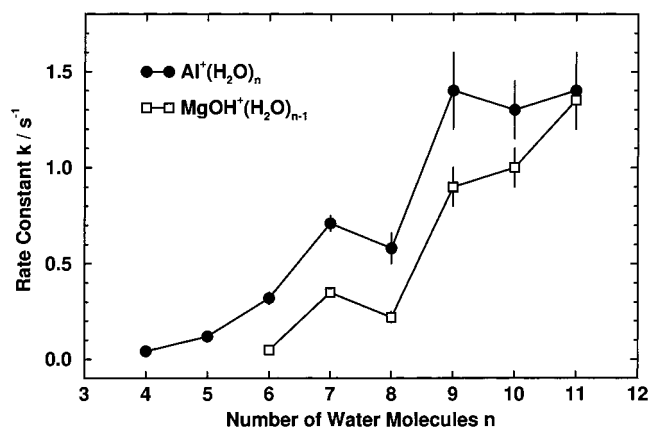


Figure 4. Rate constants for water loss from $\text{Al}^+(\text{H}_2\text{O})_n$ and $\text{MgOH}^+(\text{H}_2\text{O})_{n-1}$ hydrated aluminum and magnesium hydroxide ions. For the same n , these species differ in only one hydrogen atom. The rate constants run parallel for $n = 6\text{--}9$, which indicates similar structural features that cause the relatively low value at $n = 8$. The $\text{MgOH}^+(\text{H}_2\text{O})_{n-1}$ values are taken from ref 21.

is sufficient to gradually drive a small fraction of the clusters over the barrier for water loss.

The size dependence of the intracuster reaction rate constants is also not easy to explain, and it is useful to discuss the four previously suggested mechanisms^{21a,22} in light of the present data. Importance of a clathrate structure associated with a magic size of 20 molecules may be safely ruled out. In the first place, one might argue that a particularly stable and rigid hydrate structure would reduce, rather than enhance the intracuster reaction rate, while experimentally, a broad reactivity maximum centered around $n = 20$ is observed. There is also a local maximum for H_2 formation at $n = 13$, even though there is no obvious self-contained closed-shell structure of an Al^+ cation with 13 water molecules. Furthermore, clathrate structures in bulk water tend to form around hydrophobic centers at high

pressures, while Al^+ is surely hydrophilic, and the clusters are present in ultrahigh vacuum.

Neutral aluminum is known to insert into the water $\text{O}\text{--}\text{H}$ bond,³⁷ and the same may surely be possible for the aluminum cation. It has, in fact, been calculated that $\text{HAIOH}^+(\text{H}_2\text{O})_n$ species lie lower in energy than the noninserted ones, but the insertion is associated with an activation barrier. For nonsolvated HAIOH^+ ion, this barrier was calculated to be 267 kJ/mol,³⁸ but this value may be lowered considerably on hydration. On the other hand, metal insertion into a covalent bond usually requires free coordination sites on the metal. In the size range around $n = 20$, however, where the observed H_2 formation is most efficient, the aluminum is almost surely fully coordinated. One can, however, imagine that the insertion already takes place upon solvation of the Al^+ in the ion source, where presumably an Al^+ laser-ablated ion is taken in by a preformed water cluster and the clusters actually possess $\text{HAIOH}^+(\text{H}_2\text{O})_n$ structures. One would, however, still have to face the problem of why the hydride decomposes preferentially in hydrated clusters around $n = 20$. This and similar structural questions could be answered unambiguously by direct spectroscopic studies.

To explain the fragmentation of $\text{Mg}^+(\text{H}_2\text{O})_n$ clusters and the evolution of atomic hydrogen it was suggested that their actual structure is $\text{Mg}^{2+}(\text{H}_2\text{O})_n\text{e}^-$, with a hydrated Mg^{2+} ion and a hydrated electron.^{20,21} While this explanation works rather well in the magnesium system, it is less satisfactory in the case of aluminum. Simple thermochemistry suggests that further ionization of Mg^+ in water should be an exothermic process, but similar considerations for Al^{3+} formation are much less conclusive.^{21a} As one would expect, the onset of hydrogen formation occurs at higher values of n for aluminum relative to magnesium, but the region where hydrogen formation occurs is much broader. One would expect that two hydrated electrons were more readily destabilized in the shrinking cluster, and thus, the persistence of $\text{Al}^+(\text{H}_2\text{O})_n$ clusters and of hydrogen formation

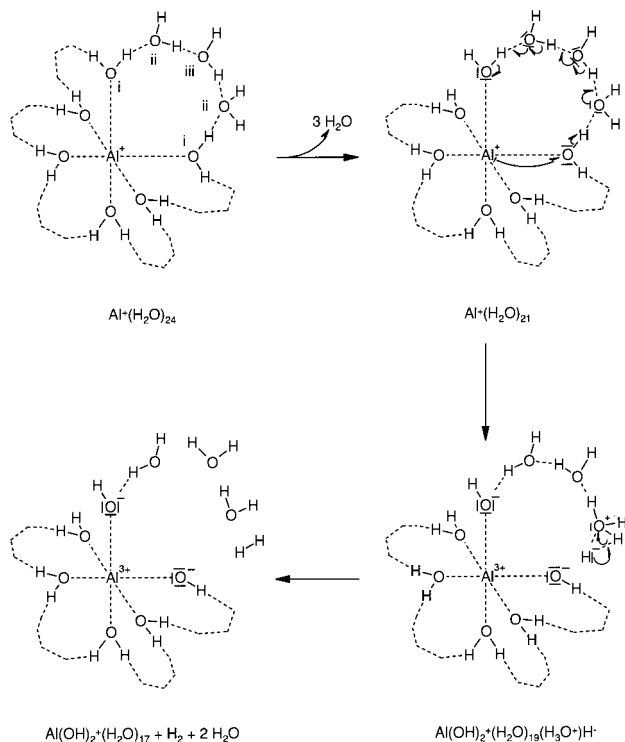


Figure 5. Proposed mechanism of hydrogen formation in Al⁺(H₂O)_n. Assuming a hexacoordinated aluminum cation, there are 6 water molecules in the first (i) solvation shell, which are connected by 12 H₂O in the second (ii) and 6 H₂O in the third (iii) solvation shell, resulting in $n = 24$, the onset of the hydrogen formation. For clarity, only one of the six chains of water molecules is shown in detail. When three water molecules, i.e., one chain, evaporate, Al⁺(H₂O)₂₁ is reached, where hydrogen formation is most efficient. The first step is a concerted rearrangement of lonepairs, leading to the OH⁻-Al³⁺-OH⁻ saltbridge entity together with a transient H⁻-H₃O⁺ ion pair. The ion pair recombines immediately, releasing H₂ and two to three water molecules, driven by the reaction enthalpy.

at $n = 11-15$, a region where the transformation process is completed in the magnesium case, would seem to argue against the solvated electron hypothesis. The kinetics of the intracuster processes in the hydrated aluminum clusters differs greatly from that in the magnesium system, and a transfer of the explanation is not necessarily successful.

One can find a way to make the size dependence plausible with the help of the previously suggested proton-transfer mechanism.²² If one assumes Al⁺ to be hexacoordinated, as on the basis of ¹⁷O NMR studies Al³⁺ is in aqueous solutions,³⁹ there would be 6 H₂O in the first solvation shell and 12 in the second. In the third shell, one could imagine an additional 6 water molecules stabilizing the cluster by linking pairs of the second-shell ligands, as shown in Figure 5, with about 24 water molecules being needed to complete a stable third solvation shell. This coincides with the onset of hydrogen formation. Coming from larger sizes, one observes the onset of the reaction around $n = 24$, reaching a maximum near $n = 20$ or 21. Removing three water molecules from $n = 24$ leaves an Al⁺(H₂O)₂₁ cluster with two partly unsolvated water molecules in the first solvation shell. By a series of electron pair shifts along one of the five water molecule loops, as shown in the figure, one obtains a charge distribution approximated by Al³⁺-OH⁻-H⁻-H₃O⁺•H₂O-H₂O-OH⁻(-Al³⁺). The H⁻/H₃O⁺ ion pair can then recombine, forming H₂ and H₂O. The maximum of the intracuster reaction at $n = 20$ and $n = 21$ could indicate that partly unsolvated first-shell water molecules are promoting the intracuster reaction, and clusters of these sizes would

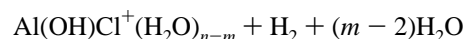
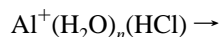
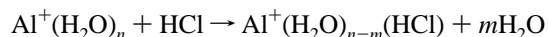
combine the availability of partly unsolvated first-shell water molecules with a maximum number of five sites of water chains that are required for proton transfer, as indicated in the figure. For smaller clusters, there are fewer chains between first-shell water molecules and hydrogen formation becomes less and less probable until it ultimately ceases around $n = 11$. The arguments are also valid if the Al⁺ ion is tetracoordinated instead of hexacoordinated, and do not rely on the Al⁺ ion being in a central position within the cluster. The key ideas are that a minimum number of water molecules is needed for the formation of three- to five-membered chains of water molecules and that, beyond a critical size, which happens to be $n \approx 24$, evaporation of water molecules is much more efficient than hydrogen formation, probably for kinetic reasons. Proton transfer through a chain of water molecules has recently been investigated in theoretical works⁴⁰⁻⁴² and has been found to lower the activation energy for proton-transfer reactions significantly, if the chain was three or four water molecules long. The observations presented here indicate that proton transfer through short chains of water molecules may play an important role in cluster as well as condensed-phase chemistry.

One can, however, envision a combination of the bond insertion and the proton-transfer mechanism. If the clusters emerge from the source as HAlOH⁺(H₂O)_n species, one can think of a solvation-dependent deprotonation, whereby H-Al-(III)-OH⁺(H₂O)_n is converted into Al(I)-OH(H₂O)_n(H⁺) upon sufficient addition of water, which would replace the step of H₃O⁺ formation in Figure 5. The deprotonation may be driven by the presumably decreasing Al-H bond strength with increasing solvation, relative to the energy gained by the formation of an extended (H₂O)_nH⁺ network.

Reactions of Al⁺(H₂O)_n and Al(OH)₂⁺(H₂O)_m with HCl Hydrogen Chloride. Highly instructive are the reactions of the hydrated aluminum clusters. To investigate their reactivity with hydrogen chloride, we have introduced gaseous HCl into the ultrahigh vacuum region at a constant pressure of 1.2×10^{-7} mbar, amounting to roughly 10 collisions s⁻¹. We then injected a cluster distribution spanning the desired size region and recorded the mass spectra after varying reaction delays. The final outcome of the reactions was quite different, depending on the initially selected size distribution.

When small Al⁺(H₂O)_n clusters, with $n \leq 11$ were initially selected, regardless of reaction delay, no chemical reaction was observed. The only effect of the HCl presence was a slightly increased rate of fragmentation, which now includes in addition to the blackbody radiation also a contribution of collisional processes. Like in the absence of collisions or when an inert collision gas was used, the final product after 20 s was mainly the $n = 4$ cluster, fragmenting only very slowly further to $n = 3$.

In contrast to the smaller species, clusters with more than 11 water ligands react very efficiently with HCl. A ligand exchange, replacing one or two water molecules with an HCl ligand, is very rapidly followed by an intracuster reaction with elimination of molecular hydrogen and probably loss of additional water ligands



The rate of the second step of this reaction sequence depends on the number of water ligands in the cluster. For smaller

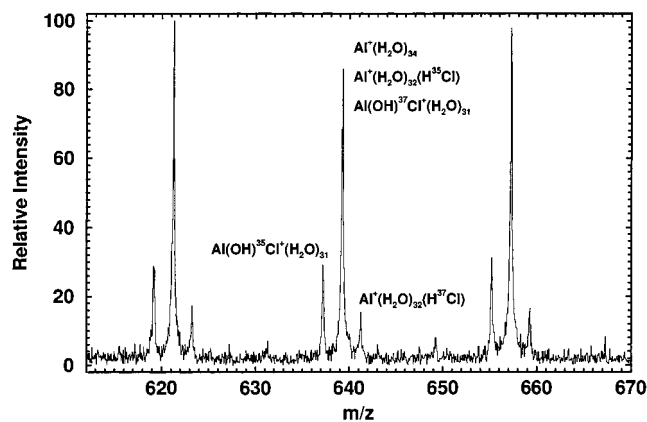
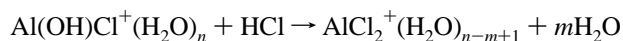


Figure 6. Typical part of a mass spectrum of the reaction of large $\text{Al}^+(\text{H}_2\text{O})_n$ hydrated aluminum cations with HCl hydrogen chloride, with a reaction delay of 0.2 s at an HCl pressure of 1.2×10^{-7} mbar. $\text{Al}^+(\text{H}_2\text{O})_{34}$ has the nominal mass of 639. The presence of the peak at mass 641 indicates the presence of $\text{Al}^+(\text{H}_2\text{O})_{32}(\text{HCl})$; that is two H_2O molecules are replaced by one HCl. The peak at mass 637 is due to a reaction product that has evaporated H_2 molecular hydrogen; that is the presence of $\text{Al}(\text{OH})\text{Cl}^+(\text{H}_2\text{O})_{31}$ indicates that introducing HCl into the cluster removes the upper size limit for hydrogen formation. The peaks also contain a small fraction of secondary reaction products, where additional water molecules are replaced by HCl. The two isotopes of chlorine and their relative abundance, however, allow for the unambiguous identification of the primary reaction steps.

species, it appears to be almost immediate, but for larger species above $n \approx 25$, the intermediate $\text{Al}^+(\text{H}_2\text{O})_n(\text{HCl})$ species are stable enough to be detected (Figure 6). From the relative intensities of the intermediate and the product after the H_2 elimination, $\text{Al}(\text{OH})\text{Cl}^+(\text{H}_2\text{O})_m$, one can roughly estimate the lifetime of these large ligand-exchange $\text{Al}^+(\text{H}_2\text{O})_n(\text{HCl})$ products to be of the order of 100 ms. Although the intracuster reaction rate decreases with cluster size, it is efficient for clusters within the entire range studied (up to $n \approx 50$), and no upper limit was observed.

Subsequent collisions then lead to replacement of the remaining hydroxyl anion by Cl^- , with the HCl proton apparently recombining with OH^- to yield an additional water ligand



The chloride-containing cluster may then exchange the water ligands and “dissolve” further HCl molecules. However, like in the case of pure protonated clusters,^{16b} this uptake of additional molecules of hydrogen chloride is limited and depends on cluster size. A certain minimum number of water molecules is needed to dissolve and ionize each HCl molecule. This can best be seen if one follows not only the formation of the clusters of the type $\text{AlCl}_2^+(\text{H}_2\text{O})_n(\text{HCl})_m$, that is, containing both water and HCl, but also their subsequent gradual fragmentation, either by blackbody radiation or by collisions.

Figure 7 shows a cluster distribution after a relatively long reaction delay of about 4 s, when the clusters are effectively “saturated” with HCl. One can note that the number of HCl molecules in a given cluster is not arbitrary but changes with n . We have shown previously that also in hydrated proton and MgCl^+ clusters,^{16b,21b} solvation of each HCl molecule requires a certain minimum number of water molecules. In the present case of $\text{AlCl}_2^+(\text{H}_2\text{O})_n(\text{HCl})_m$ clusters, $n \geq 9$; that is, at least nine water molecules are necessary for $m = 1$, and $n \geq 19$ is needed for $m = 2$, that is to dissolve two additional HCl

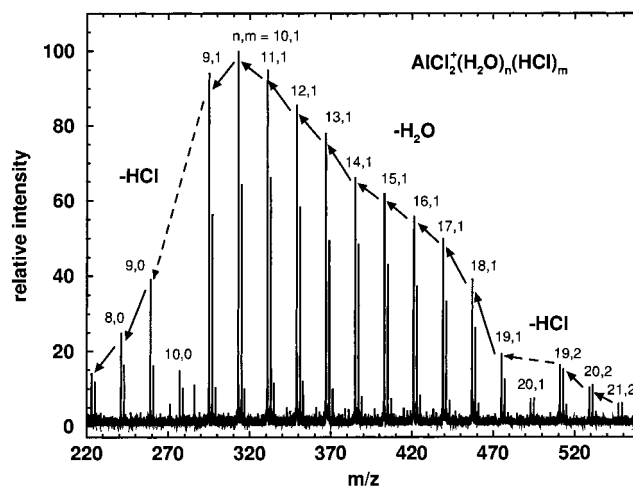


Figure 7. Typical part of a mass spectrum of the reaction of large $\text{Al}^+(\text{H}_2\text{O})_n$ hydrated aluminum cations with HCl, taken with a reaction delay of 4 s and otherwise similar conditions as those described in Figure 6. The clusters are basically saturated with HCl and can be written as $\text{AlCl}_2^+(\text{H}_2\text{O})_n(\text{HCl})_m$. Collisionally and blackbody radiation induced dissociation are the dominant processes leading to evaporation of either HCl or H_2O as indicated by the arrows. Loss of HCl preferentially occurs at $n = 19$ and $n = 9$ water molecules, indicating that solvation of a $\text{Cl}^- - \text{H}^+$ ion pair breaks down.

molecules. During the cluster fragmentation, the hydrated clusters gradually lose the water ligands, but whenever one of the above limits is reached, a proton within the cluster recombines with a chloride ion to form covalent hydrogen chloride. The HCl molecule with a single proton is more weakly bound than H_2O and evaporates from the cluster in the next step rather than a water molecule, as shown schematically by arrows in Figure 7. Finally, after the longest decay studied, that is, about 100 s, roughly equal amounts of $\text{AlCl}_2^+(\text{H}_2\text{O})_3$ and $\text{AlCl}_2^+(\text{H}_2\text{O})_4$ remain in the spectrum.

Interesting is the presence of a lower limit for the reactions of $\text{Al}(\text{H}_2\text{O})_n^+$ with HCl and the absence of any reactivity of clusters with $n < 11$. The intracuster reaction in this case is essentially equivalent to dissolving a metal in acids. It involves oxidation of the aluminum atom with a concurrent reduction of a proton to hydrogen and can be viewed as a proton-catalyzed reaction. As discussed above, some minimum number of water ligands is needed to accomplish the ionization of HCl into Cl^- and H^+ . In clusters with an insufficient number of water ligands, this dissociation cannot take place and the proton needed for the reaction is thus not available.

It is observed that introducing a single HCl molecule into the cluster removes the upper but not the lower limit for the intracuster reaction that leads to formation of molecular hydrogen. The intracuster reaction is induced upon dissolving an HCl molecule in the cluster into solvated H^+ and Cl^- . Concerning the mechanisms we have discussed before, there is no obvious reason that the presence of these ionic species in the solvation shell should promote the OH bond insertion mechanism and shift or even completely remove the upper limit for the intracuster reaction. The proton-transfer mechanism, on the other hand, can very well be promoted by the presence of additional ions in the cluster. Dissolving an HCl molecule means introducing a $\text{Cl}^-/\text{H}_3\text{O}^+$ ion pair into the cluster. Both ions have a certain mobility in the cluster, and on a time scale of 100 ms, Cl^- may come in contact with the Al^+ ion and induce the shift of lone pairs which results in the $\text{Cl}^- - \text{Al}^{3+} - \text{OH}^-$ salt bridge and the $\text{H}^- - \text{H}_3\text{O}^+$ ion pair, as indicated

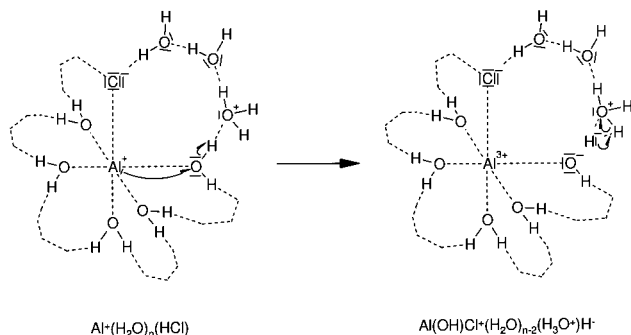
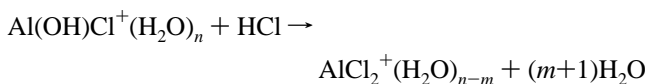
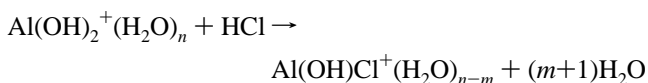


Figure 8. Mechanism of hydrogen formation in Al⁺(H₂O)_n(HCl) clusters. HCl is dissolved, forming H₃O⁺ and Cl⁻ in the cluster. On a time scale of 100 ms, Cl⁻ comes in contact with the Al⁺ ion and induces the shift of lone pairs, which results in the Cl⁻–Al³⁺–OH⁻ salt bridge and the H⁻–H₃O⁺ ion pair. Analogous to the case in Figure 5, recombination leads to elimination of H₂ molecular hydrogen and additional water molecules.

in Figure 8. Analogous to Figure 5, recombination leads to elimination of H₂ molecular hydrogen and additional water molecules.

We have also investigated the reactions of the hydroxide clusters Al(OH)₂⁺(H₂O)_n with HCl, and here, the situation is considerably simpler. Regardless of the number of water ligands, the reaction with water simply involves sequential replacing of the two OH⁻ anions by chlorides, Cl⁻



The solvation of additional HCl molecules then shows the size dependence described above, as the same stoichiometry is reached regardless of whether the intracuster reaction occurs before or after the intake of the first HCl molecule.

Conclusion

Both the size dependence of the intracuster reaction driven by blackbody radiation and the wiping out of the upper limit for the intracuster reaction by solvation of HCl in the cluster are strong evidence for the concerted proton-transfer mechanism suggested previously. The formation of hydrogen is thus interpreted in terms of basic chemical concepts. To further investigate the mechanism of hydrogen formation in Al⁺(H₂O)_n hydrated aluminum clusters, it is first of all necessary to sort out the structure and connectivity of Al⁺(H₂O)_n, $n = 4-30$, by spectroscopic experiments and ab initio or molecular mechanics calculations. Electronic spectroscopy could probe the oxidation state of aluminum in Al(I)⁺(H₂O)_n versus HAl(III)OH⁺(H₂O)_{n-1}. Temperature-resolved studies of the intracuster reaction may yield activation energies and frequency factors and thus be the basis for a theoretical model of this rather complex intracuster reaction.

Acknowledgment. The authors thank the referee for valuable suggestions and helpful comments. Financial support by the Deutsche Forschungsgemeinschaft through the Schwerpunktprogramm Molekulare Cluster and the SFB 377: Photoionization und Ladungstrennung in grossen Molekülen, Clustern und

in kondensierter Phase, and the Fonds der Chemischen Industrie is gratefully acknowledged.

References and Notes

- (1) Velegrakis, M.; Lüder, C. *Chem. Phys. Lett.* **1994**, *223*, 139.
- (2) (a) Woodward, C. A.; Dobson, M. P.; Stace, A. J. *J. Phys. Chem.* **1996**, *100*, 5605. (b) *J. Phys. Chem. A* **1997**, *101*, 2279.
- (3) Beyer, M.; Berg, C.; Albert, G.; Achatz, U.; Bondybey, V. E. *Chem. Phys. Lett.* **1997**, *280*, 459.
- (4) Buthelezi, T.; Bellert, D.; Hayes, T.; Brucat, P. J. *Chem. Phys. Lett.* **1996**, *262*, 303.
- (5) Scurlock, C. T.; Pilgrim, J. S.; Duncan, M. A. *J. Chem. Phys.* **1995**, *103*, 3293.
- (6) (a) Dzidic, I.; Kebarle, P. *J. Phys. Chem.* **1970**, *74*, 14664. (b) Kebarle, P. *Annu. Rev. Phys. Chem.* **1977**, *28*, 445.
- (7) Keesee, R. G.; Castleman, A. W. *J. Phys. Chem. Ref. Data* **1986**, *15*, 1011.
- (8) (a) Jayaweera, P.; Blades, A. T.; Ikononou, M. G.; Kebarle, P. *J. Am. Chem. Soc.* **1990**, *112*, 2452–2454. (b) Blades, A. T.; Jayaweera, P.; Ikononou, M. G.; Kebarle, P. *J. Chem. Phys.* **1990**, *92*, 5900–5906. (c) *Int. J. Mass Spectrom. Ion Proc.* **1990**, *101*, 325. (d) *Int. J. Mass Spectrom. Ion Proc.* **1990**, *102*, 251.
- (9) (a) Spears, K. G.; Fehsenfeld, F. C.; McFarland, M.; Ferguson, E. *J. Chem. Phys.* **1972**, *56*, 2562. (b) Spears, K. G.; Fehsenfeld, F. C. *J. Chem. Phys.* **1972**, *56*, 5698.
- (10) Rodriguez-Cruz, S. E.; Jockusch, R. A.; Williams, E. R. *J. Am. Chem. Soc.* **1998**, *120*, 5842.
- (11) (a) Bauschlicher, C. W., Jr.; Langhoff, S. R.; Partridge, H.; Rice, J. D.; Komornicki, A. *J. Chem. Phys.* **1991**, *95*, 5142. (b) Bauschlicher, C. W., Jr.; Partridge, H. *J. Chem. Phys.* **1991**, *95*, 9694.
- (12) Watanabe, H.; Iwata, S. *J. Phys. Chem.* **1996**, *100*, 3377.
- (13) Dalleska, N. F.; Tjelja, B. L.; Armentrout, P. B. *J. Phys. Chem.* **1994**, *98*, 4191.
- (14) Selegue, T. J.; Moe, N.; Draves, J. A.; Lisy, J. M. *J. Chem. Phys.* **1992**, *96*, 7268.
- (15) Achatz, U.; Joos, S.; Berg, C.; Schindler, T.; Beyer, M.; Albert, G.; Niedner-Schatteburg, G.; Bondybey, V. E. *J. Am. Chem. Soc.* **1998**, *120*, 1876.
- (16) (a) Achatz, U.; Joos, S.; Berg, C.; Beyer, M.; Niedner-Schatteburg, G.; Bondybey, V. E. *Chem. Phys. Lett.* **1998**, *291*, 459. (b) Schindler, T.; Berg, C.; Niedner-Schatteburg, G.; Bondybey, V. E. *Chem. Phys. Lett.* **1994**, *229*, 57.
- (17) Castleman, A. W., Jr. *Int. J. Mass Spectrom. Ion Proc.* **1992**, *118/119*, 167.
- (18) Schindler, T.; Berg, C.; Niedner-Schatteburg, G.; Bondybey, V. E. *J. Chem. Phys.* **1996**, *104*, 3998.
- (19) Albert, G.; Berg, C.; Beyer, M.; Achatz, U.; Joos, S.; Niedner-Schatteburg, G.; Bondybey, V. E. *Chem. Phys. Lett.* **1998**, *291*, 459.
- (20) (a) Fuke, K.; Misaizu, F.; Sanekata, M.; Tsukamoto, K.; Iwata, S. *Z. Phys. D* **1993**, *26* (Suppl.), S180. (b) Watanabe, H.; Iwata, S.; Hashimoto, K.; Misaizu, F.; Fuke, K. *J. Am. Chem. Soc.* **1995**, *117*, 755. (c) Watanabe, H.; Asada, T.; Iwata, S. *Bull. Chem. Soc. Jpn.* **1997**, *70*, 2619.
- (21) (a) Berg, C.; Achatz, U.; Beyer, M.; Joos, S.; Albert, G.; Schindler, T.; Niedner-Schatteburg, G.; Bondybey, V. E. *Int. J. Mass Spectrom. Ion Proc.* **1997**, *167/168*, 723. (b) Berg, C.; Beyer, M.; Achatz, U.; Joos, S.; Niedner-Schatteburg, G.; Bondybey, V. E. *Chem. Phys.* **1998**, *239*, 379.
- (22) Beyer, M.; Berg, C.; Görlitzer, H. W.; Schindler, T.; Achatz, U.; Albert, G.; Niedner-Schatteburg, G.; Bondybey, V. E. *J. Am. Chem. Soc.* **1996**, *118*, 7386.
- (23) Harms, A. C.; Khanna, S. N.; Chen, B.; Castleman, A. W., Jr. *J. Chem. Phys.* **1994**, *100*, 3540.
- (24) Selegue, T. J.; Lisy, J. M. *J. Am. Chem. Soc.* **1994**, *116*, 4874.
- (25) Lu, W. Y.; Yang, S. H. *J. Phys. Chem. A* **1998**, *102*, 825.
- (26) Schindler, T.; Berg, C.; Niedner-Schatteburg, G.; Bondybey, V. E. *Chem. Phys. Lett.* **1996**, *250*, 57.
- (27) Dunbar, R. C.; McMahon, T. B. *Science* **1998**, *279*, 194.
- (28) Sena, M.; Riveros, J. M. *Rapid Commun. Mass Spectrom.* **1994**, *8*, 1031.
- (29) Schnier, P. D.; Price, W. D.; Jockusch, R. A.; Williams, E. R. *J. Am. Chem. Soc.* **1996**, *118*, 7178.
- (30) Bondybey, V. E.; Schindler, T.; Berg, C.; Beyer, M.; Achatz, U.; Joos, S.; Niedner-Schatteburg, G. In *Recent Theoretical and Experimental Advances in Hydrogen-Bonded Clusters*; NATO ASI Series; Xantheas, S. S., Ed.; Kluwer: Dordrecht, in press.
- (31) Cofer, W. R., III; Bendura, R. J.; Sebacher, D. I.; Pellett, G. L.; Gregory, G. L.; Maddrea, G. L., Jr. *AIAA J.* **1985**, *23*, 283.
- (32) Misaizu, F.; Sanekata, M.; Fuke, K. *Z. Phys. D* **1993**, *26*, S177.
- (33) Berg, C.; Schindler, T.; Niedner-Schatteburg, G.; Bondybey, V. E. *J. Chem. Phys.* **1995**, *102*, 4870.
- (34) (a) Bondybey, V. E.; English, J. H. *J. Chem. Phys.* **1981**, *74*, 6978. (b) Dietz, T. G.; Duncan, M. A.; Powers, D. E.; Smalley, R. E. *J. Chem. Phys.* **1981**, *74*, 6511.

- (35) Coe, J. C. *J. Phys. Chem. A* **1997**, *101*, 2055.
- (36) Combariza, J. E.; Kestner, N. R.; Jortner, J. *J. Chem. Phys.* **1994**, *100*, 2851.
- (37) (a) Hauge, R. H.; Kauffman, J. W.; Margrave, J. L. *J. Am. Chem. Soc.* **1980**, *102*, 6005. (b) Sakaki, S.; Jordan, K. D. *J. Phys. Chem.* **1993**, *97*, 8917.
- (38) Hrušák, J.; Stöckigt, D.; Schwarz, H. *Chem. Phys. Lett.* **1994**, *221*, 518.
- (39) Fratiello, A.; Lee, R. E.; Nishida, V. M.; Schuster, R. E. *J. Chem. Phys.* **1968**, *48*, 3705.
- (40) Siegbahn, P. E. M. *J. Phys. Chem.* **1996**, *100*, 14672.
- (41) Nguyen, M. T.; Raspoet, G.; Vanquickenborne, L. G.; van Duijnen, P. T. *J. Phys. Chem. A* **1997**, *101*, 7379.
- (42) Aida, M.; Yamataka, H.; Dupuis, M. *Chem. Phys. Lett.* **1998**, *202*, 474.